Hot and cold spots of pest-induced US urban tree death, 2020-2050.

Authors

Emma J. Hudgins[1*], Frank H. Koch[2], Mark J. Ambrose[3], Brian Leung[1,4]

Affiliations

[1] Dept. of Biology, McGill University.

[2] USDA Forest Service, Southern Research Station.

[3] Dept. of Forestry and Environmental Resources, North Carolina State University.

[4] School of Environment, McGill University.

*Corresponding author, Stewart Biology Building, 1205 avenue Docteur Penfield, Montreal, Quebec, Canada, H3A 1B1, tel: +15142452054, emma.hudgins@mail.mcgill.ca

Short title: US urban pest impacts, 2020-2050

Keywords: Forest ecology, Economic impact, Scenario modelling, Invasive species, Invasive insects, Street trees, Emerald ash borer

Article Type: Research article

Statement of authorship: EJH and BL conceptualized the study. EJH performed the analyses and created the figures. EJH, BL, FHK and MJA wrote the paper. FHK and MJA provided insect and urban tree expertise and commented on realism of results. MJA manages the urban tree database.

Data availability statement: All data and code used in the analyses (privacy restrictions permitting) are available at www.github.com/emmajhudgins/UStreedamage. A Zenodo DOI will be provided at the time of acceptance.

Conflict of interest: The authors have no conflicts of interest to declare.

Abstract

1. Urban trees are important nature-based solutions for future wellbeing and livability but are at high risk of mortality from insect pests. United States (US) urbanization levels are already at 82% and are growing, making urban tree mortality a matter of concern for the majority of its population. Until now, the magnitudes and spatial distributions of risks were unknown.

2. Here, we combine new models of street tree populations in ~30,000 US communities, species-specific spread predictions for 57 invasive insect species, and estimates of tree death due to insect exposure for 48 host tree genera.

3. We estimate that an additional 1.4 million street trees will be killed by insects from 2020 through 2050, costing an annualized average of US$ 30M. However, these estimates hide substantial variation: 23% of urban centers will experience 95% of all insect-induced mortality. Further, 90% of all mortality will be due to emerald ash borer (*Agrilus planipennis,* EAB), which is expected to kill virtually all ash trees (*Fraxinus* spp.) in >6000 communities.

4. We define an EAB high-impact zone spanning 902,500km^2, largely within the southern and central US, within which we predict the death of 98.8% of all ash trees. “Mortality hotspot cities” include Milwaukee, WI, Chicago, IL, and New York, NY.

5. We identify Asian wood borers of maple and oak trees as posing the highest future risk to US urban trees, where a new establishment could cost US$ 4.9B over 30 years.

6. *Policy implications:* To plan effective mitigation, managers need to know which tree species in which communities will be at the greatest risk, as well as the highest-risk

insects. We provide the first country-wide, spatial forecast of urban tree mortality due to invasive insect pests. This framework identifies dominant pest insects and spatial impact hotspots, which can provide the basis for spatial prioritization of spread control efforts such as quarantines and biological control release sites. Further, these findings produce a list of biotic and spatiotemporal risk factors for future high-impact US urban forest insect pests.

Introduction

Previous analyses suggest that urban tree impacts will comprise the dominant share of economic damages caused by invasive alien forest insects (IAFIs) in the United States (US) (Aukema et al. 2011). Urban tree populations include highly susceptible species like ash (*Fraxinus* spp.) that are being decimated by emerald ash borer (EAB, *Agrilus planipennis*) (Kovacs et al. 2010). To eliminate the potential for injury or property damage due to dead trees, infested urban trees must be treated or removed (Fahrner et al. 2017). Moreover, the importance of urban forests is only expected to grow. While urbanization is already very high in the US (82% in 2018), it has not yet reached saturation (World Bank, http://data.worldbank.org, UN DESA, http://population.un.org). At the same time, there has been a push for urban 'greening' (i.e., increasing urban forest canopy). Urban trees perform many important ecosystem services, including lowering cooling costs (Norton et al. 2015), buffering against flooding, increasing air quality, carbon sequestration, improving citizens' mental and physical health outcomes, and creating important habitat (Van den Berg et al. 2010; Roy et al. 2012). The high tree mortality risk posed by IAFIs can greatly diminish these myriad benefits.

While IAFI life histories differ, they are known to be transported long distances by humans (Hulme 2009), potentially with similar drivers across entire dispersal pathways (Hudgins et al. 2017, 2020). Thus, the creation of a pathway-level damage estimate can provide insight into the benefit of limiting future spread via these pathways (e.g. through quarantines, highway checkpoints to limit firewood movement). Past estimates of IAFI damage have been important in providing support for phytosanitary

measures such as ISPM15 (IPPC 2002), a wood packing material treatment protocol, whose adoption is growing worldwide (Leung et al. 2014). A previous pathway-level estimate for the cumulative cost of all US IAFIs was performed a decade ago and had substantial data limitations (Aukema et al. 2011). Since then, contemporary advances allow direct estimates of spread for every IAFI species as well as host prevalence and IAFI-induced mortality for every tree species in every community across the United States. This allows not only the estimation of country-wide IAFI damages, but also IAFI and host-specific damages and their spatial distribution. Further, we can examine the impact of tree mortality dynamics on cost dynamics and derive better risk assessments of not-yet established pests, based their functional traits and host distributions.

In this paper, we synthesized four subcomponents of IAFI invasions: 1) a model of spread for 57 IAFI species, 2) a model for the distribution of all urban street tree host genera across all US communities, 3) a model of host mortality in response to IAFI-specific infestation for all urban host tree species, and 4) the cost of removing and replacing dead trees, to provide the best current estimate of the damage to street trees, including explicit estimates for all known IAFIs across all major insect guilds.

Materials and Methods

We synthesized four subcomponent models of IAFI invasions (see conceptual diagram, Fig. S1).

IAFI dispersal forecasts

We modelled spread using the Semi-Generalized Dispersal Kernel (SDK, Hudgins et al. 2020). This is a spatially explicit, negative exponential dispersal kernel model that can account for additional spatial predictors in source and recipient sites. The SDK builds from the Generalized Dispersal Kernel (GDK, Hudgins et al. 2017) as a starting point, using human population density, forested land area and tree density in source and destination sites as moderators of spread. The SDK combines up to three species-specific corrections for each species to maximize predictive ability: 1) a species-specific intercept term, 2) information on an IAFI's likely initial invasion location, and 3) niche-related limitations when evidenced in the literature. The SDK was applied to all 57 IAFIs believed to cause some damage from Aukema et al. (2011) and projected from 2020 to 2050 (Fig. S2).

Street tree models

Our fitting set consisted of 653 street tree databases for US communities where street tree inventory data had been collected (Fig. S3, Koch et al. 2018). In two communities (Tinley Park and, IL and Fort Wayne, IN), preventative cutting for EAB was conducted prior to the most recent inventory and was therefore accounted for within our dataset. We modelled the abundance and diameter at breast height (DBH) for trees within each genus, as treatment costs are dependent on number and diameter of trees (Aukema et al. 2011). We split trees into three diameter classes (small = 0-30cm, medium = 31-60cm, large

128 >60cm). We first fit models for the total tree abundance of all species by diameter class,
129 and then used these total tree models to help predict genus-specific tree abundance within
130 each diameter class. Street tree inventory data are not always reliably reported to the
131 species level across municipalities, and some species are so rare in street tree inventories
132 that it would have been very difficult to develop robust species-level models, so we
133 limited our examination to the genus level. Since IAFIs may not be equally impactful to
134 all host tree species in a genus, we had to estimate the genus-level severity of each IAFI
135 species for each IAFI-host combination. We did so by estimating the species-level
136 breakdown of each genus based on their average relative proportions across our 653
137 inventoried communities, and assuming this distribution was representative in other
138 projected communities.

139 We modelled the total abundance of street trees in a community using boosted
140 regression trees (BRT, *gbm.step* within R package *dismo*, Hijmans et al. 2017, Appendix
141 S1) relating the logarithmically-scaled total tree abundance within a diameter class to
142 community-specific predictors, employing environmental variables from WORLDCLIM
143 (Fick & Hijmans 2017) and community characteristics used in Koch et al. (2018), and
144 sourced largely from the National Land Cover Database (NLCD, Homer et al. 2015), the
145 US Census and the American Community Survey (https://www.census.gov/data.html,
146 Table S1).

147 Next, we estimated the abundance of street trees within each genus, using the
148 same climatic and demographic factors as the total tree abundance model as well as the
149 total tree abundance model output as predictors (Fig. S1). We considered two approaches:
150 1) zero-inflated Poisson generalized additive models (GAMs), or 2) a two-step BRT

151 approach. We compared BRT and GAM models that were fit to all genera simultaneously
152 (general BRT/GAM models using genus-specific intercept terms) with models that were
153 fit to each genus separately (customized BRT/GAM models) (Fig. S1). We chose the
154 model that produced the strongest relationship for each genus using R^2 values that were
155 relative to the 1:1 line (i.e, a normalized mean squared error, R^2_{MSE}, Appendix S1).

156 We synthesized the previous two modelling steps, intersecting IAFI spread
157 forecasts with predicted tree distributions (using observed tree data where available), to
158 create forecasts of tree exposure, which we define as the sum of predicted density of each
159 IAFI species, multiplied by their predicted host tree abundance in each community.

160

161 Host mortality model

162

163 We examined the impacts of the three major feeding guilds of IAFIs (Aukema et al.
164 2010): Foliage feeders included insects that feed on leaf or needle tissue. Sap feeders
165 included all species that consume sap, including scale insects and gall-forming species.
166 Borers included species that feed on phloem, cambium, or xylem. Across insect guilds,
167 the logic from Aukema et al. (2011) appeared to hold: most species were innocuous, but a
168 small number caused high mortality (Table S7). In contrast, while several invasive
169 pathogens were mentioned in Potter et al. (2019), pathogens are only reliably reported
170 when they produce noticeable impacts (Aukema et al. 2011). To avoid mischaracterizing
171 their impacts, we removed pathogens from the remainder of our analysis.

We ranked the severity of a given IAFI infestation on a particular host using a scale based on observed long-term percent mortality (Table S7, defined in Potter et al. 2019). We fit a Beta distribution to the frequency distribution of IAFI-host interactions in each of these categories using Stan (Carpenter et al. 2017), a program and language for efficient Bayesian estimation. We used the posterior mean of each severity class as the expected mortality for an IAFI-host interaction within each category.

We define the term 'mortality debt' as the period between an IAFI initiating damage within a community and reaching its estimated long-term (asymptotic) host mortality within that community (see Appendix S2 for more details). While we had estimates of asymptotic mortality of host trees (Potter et al. 2019), we had no information on the rate by which trees reach this plateau. Previous estimates have ranged from 5 to 100 years (Aukema et al. 2011, Pugh 2010), so we analyzed three scenarios within this range (10, 50, 100 years). To account for what is currently known about the mortality dynamics of IAFIs within each of the feeding guilds, we focus on the most likely scenario of mortality debt across IAFI feeding guilds (10 years for borers, 50 years for defoliators, and 100 years for sap feeders). For simplicity, we assumed mortality increased by a constant fraction over time until reaching its maximum and levelling off. For example, in the 50-year mortality debt scenario, if an IAFI's maximum host mortality was defined as 90%, mortality would increase by 9% at each 5-year timestep for 10 timesteps until 90% mortality had been reached.

Management costs

As a final layer that allowed us to move from mortality estimates to cost estimates, we estimated the cost of removing and replacing dead trees. We used this cost because we believe it to be the minimum management response required, and because the extent and variability of preventive behaviour would be much harder to estimate. However, we note that this cost does not account for additional preventive cutting or any non-cutting management such as spraying or soil drenching with pesticides. We assumed that cutting was a one-time 100% effective treatment against IAFIs, or in other words, that newly planted trees were of different species and thus not susceptible to the same IAFI species that killed the previous trees. We assumed a 2% discount rate for future damages (Aukema et al. 2011) and that infestations were independent, or in other words that invasion by one IAFI did not interfere with invasion by another. This is likely a fair assumption, as there is minimal host sharing across IAFIs, and IAFI species each infest only a small proportion of hosts at a given time interval, so there is minimal potential for species interactions (Aukema et al. 2010).

We assumed the same per-tree cost estimates for cutting and replacing dead trees as in Aukema et al. (2011), where the cost of cutting increases nonlinearly with size class. If we assume that street trees are always under the jurisdiction of local governments, the cost of removal and replacement of each tree is US$450 for small trees, US$600 for medium trees, and US$1200 for large trees (these costs jump to an estimated US$600, US$800, and US$1500 for homeowners). We reported all costs incurred from 2020 to 2050 in 2019 US dollars based on a 2% discount rate relative to these baseline costs. Since these baseline per-tree management costs came from a 2011 publication, we converted them to 2019 dollars via the consumer price index, which amounted to an

218 inflation of 13.65% (World Bank, https://data.worldbank.org), though we note that the
219 present-day costs of per-tree removal may have declined with advances in technology.

220

221 Model synthesis

222

223 Once all subcomponent models had been parameterized, we synthesized the street tree
224 estimates, IAFI spread estimates, host mortality estimates, and removal costs to produce
225 overall cost estimates (Fig. S1). We summed the damages from 2020 to 2050 to obtain a
226 total discounted cost for this 30-year window. We then obtained annualized costs by
227 calculating an annuity over the 30-year time horizon using the following equation:

228 $$Annualized\ damage = D\frac{\sum_{time=min}^{max} Costs_{time}}{(1-(1+D)^{min-max})} \quad (1)$$

229 Where D is the discount rate (2%).

230 We assessed parameter uncertainty in proportional host mortality by sampling
231 from our posterior beta mortality distribution. We also used sensitivity analysis to explore
232 the effect of different mortality debt scenarios, including 1) our most likely scenario, 2)
233 setting all guilds to 10, 50, or 100-year debts, and 3) varying each guild separately while
234 holding the other two guilds at their most likely scenario. While our host distribution
235 models were based on standard modelling approaches (e.g., GAM), our Bayesian
236 formulations underlying the mortality estimates were novel and needed to be tested
237 theoretically, to ensure that parameters were identifiable, and reproduced the correct
238 behavior. See Appendix S3 for details of our theoretic analyses.

239

240 Potential impacts to non-street trees

241

242 To provide a rough estimate of non-street tree impacts, we built a model for whole-
243 community trees (i.e., street + non-street trees) from the dataset of 56 communities where
244 genus-level estimates were reported, subtracted predicted street trees from this whole
245 community estimate, and apportioned the remaining trees into residential and non-
246 residential trees based on their average fractions across all sites where land type
247 breakdowns were provided (32 municipalities).

248

249 **Results**

250

251 Urban tree pest exposure

252 Total tree abundance models were predictive with some outliers (Appendix S1, Fig. S4,
253 small trees: $R^2 = 0.78$, medium trees: $R^2 = 0.58$ large trees: $R^2 = 0.42$). Removing the
254 outliers changed the R^2 to 0.76 for small trees, 0.76 for medium trees, and 0.58 for large
255 trees. Our genus-level abundance models were strong but became slightly weaker for rare
256 genus - size class combinations (Fig. 1, overall R^2 for all genera of small trees: $R^2 = 0.93$,
257 medium trees: $R^2 = 0.93$, large trees: $R^2 = 0.92$). While relationships were variable across
258 genera, the genera that were fit most poorly did not make up a large proportion of
259 predicted trees, and none were below $R^2 = 0.25$ (Fig. S5).

260 The optimal genus-level fitting approach differed across genera depending on
261 diameter class, prevalence of genera, and whether presence/absence or tree abundance

was the response variable (Table S2). Generally, rarer genera were better fit by global BRT and GAM models, which utilized information from all other species while common species were better fit by customized models (Fig. S6). According to our models, while subject to regional variation, the population of street trees is mostly made up of maple (*Acer*) and oak *(Quercus)*, with substantial ash (*Fraxinus*, Fig. S7).

Predicted street tree exposure (measured as the number of predicted susceptible trees in Fig. 2a * IAFI relative propagule pressure in Fig. 2b, Hudgins et al. 2020) across all tree types from 2020 to 2050 was generally high in the eastern US, and only sporadically high across the western US (Fig. 2c). Predicted street tree exposure was highest among maples (*Acer* spp., 25.6M predicted exposed trees), oaks (*Quercus* spp., 5.9M), and pines (*Pinus* spp. 3.4M). The greatest number of trees were predicted to become exposed to San Jose scale (*Quadraspidiotus perniciosus,* 7.3M), Japanese beetle (*Popillia japonica,* 6.7M), and calico scale (*Eulecanium cerasorum,* 6.4M). Among residential and community trees, exposure was greatest among maples, oaks, and *Prunus* spp. (1.7B,1.1B, 707M, respectively), and the most frequently predicted IAFI encounters were with the same three species (Japanese beetle, San Jose scale, and calico scale).

Host tree mortality

The best-fitting mortality model indicated that most IAFIs fall in the low severity groups. Within all severity groups, the majority of IAFIs were at the low end of severity (Fig. 3, full results in Appendix S2). In our most likely mortality debt scenario (i.e., 10-year scenario for borers, 50-year scenario for defoliators, 100-year scenario for sap feeders,

we estimated a mortality level of 0.7-2.5% beyond expected natural mortality of street trees by 2050, where our most likely scenario fell on the higher end of this range (Table 1). Predicted street tree death varied by a factor of four based on the mortality debt scenario, with longer debts leading to lower total mortality between now and 2050 (Table 1). This was because in longer mortality debt scenarios, trees experience mortality in the years 2020-2050 from IAFIs that initially established in their communities in 2000 (50yr debt) or 1950 (100yr), but our highest impact IAFI (EAB) can only begin to cause mortality after 2002 in any scenario. Sensitivity was driven largely by wood boring species, as demonstrated by the sensitivity of mortality estimates to their mortality debt scenarios ("Vary Borers" row, Table 1). We also found that longer mortality debts led to a smoother cost curve, or costs that do not vary much due to more consistent host mortality rates (Fig. 4).

Spatially, future damages will be primarily borne in the Northeast and Midwest, driven by EAB spread (Fig. 2d). We predict that EAB will reach asymptotic mortality in 6747 new cities, which means that 98.98% of its preferred ash hosts will die. Thus, the mortality is predicted to be concentrated in a 902,500km^2 zone encompassing many major Midwestern and Northeastern cities (Fig. S10). This mortality is also predicted to result in a 98.8% loss of all ash street trees within this zone. Over 230,000 ash street trees are predicted to have died before 2020, and there are a further 69 cities where EAB is predicted to reach asymptotic mortality within 10 years of 2050 (i.e., 98.8% ash mortality by 2060). Due to the restricted range of forest ash relative to urban ash, we predict that 68% of ash trees and 76% of communities containing street ash will remain unexposed to EAB in 2060. Furthermore, at-risk ash trees are unequally distributed. We projected the

highest risk close to the leading edge of present-day EAB distributions, particularly in areas predicted to have high ash densities. The top "mortality hotspot cities", where projected additional mortality is in the range of 5,000-25,000 street trees, include Milwaukee, WI, the Chicago Area (Chicago/Aurora/Naperville/Arlington Heights, IL), Cleveland, OH, and Indianapolis, IN (Fig. 2d). Cities predicted to have high mortality outside of the Midwest include New York, NY, Philadelphia, PA, and Seattle, WA – communities with high numbers of street trees and high human population densities, which attract EAB propagules within our spread model. The states most impacted by street tree mortality match these patterns, where the highest mortality is predicted for Illinois, New York, and Wisconsin.

Cost estimates

We estimated annualized street tree costs across all guilds to be between US$29-33M per year in our most likely scenario (mean = $30M, Table 1, Fig. S11). Roughly 90% of all costs across the entire US were due to EAB-induced ash mortality. The total cost associated with street tree mortality in the top ten hotspot cities was estimated at $50M from 2020 to 2050, with $13M in Milwaukee, WI alone.

The ranking of feeding guild severity was relatively robust across mortality debt scenarios, despite the potential for differences due to the interaction of IAFI-specific spread and mortality debt dynamics. Costs were higher for longer mortality debt scenarios for borers, peaked at intermediate debt for defoliators, and peaked at the longest debt for sap feeders. These patterns were due to the relative rates of historical and

contemporary range expansion of more impactful IAFIs (i.e., high impact borers have more rapid recent range expansion, while contemporary high impact defoliator expansion is slow compared to 50 years ago). Borers were predicted to be the most damaging feeding guild ($8M-28M mean annualized street tree damages across scenarios), and EAB was consistently the top threat. Defoliators were predicted to be the second most damaging feeding guild in the next 30 years (means = $0.8M-$1.4M), despite having more widespread hosts than wood borers, due to lower asymptotic mortality levels. Defoliators had a 1-2 order of magnitude lower cost than wood-boring species, but again showed consistency in which species were the top threats within the guild. Consistent with previous work in Aukema et al. (2011), LDD moth had the highest cost of all defoliators, followed by Japanese beetle and cherry bark tortrix (*Enarmonia formosana*). The sap-feeding group accrued the lowest costs in the next 30 years due to their lower asymptotic mortality and rarer street tree hosts (mean = $0.2M-1.1M). Hemlock woolly adelgid (*Adelges tsugae*) was the highest impact sap feeder, followed by oystershell scale (*Lepidosaphes ulmi*) and elongate hemlock scale (*Fiorinia externa*). Total costs were only notably sensitive to borer mortality debt scenario misspecification (Table 1), which is promising, given our certainty of the shorter scenario for EAB.

Potential impacts to non-street trees

Mean added mortality (i.e., above background rates) for residential and non-residential community trees in the most likely scenario was 1.0% (13.3M residential and 72.1M non-residential trees, Table S10). While recognizing that non-street tree management will

likely be more variable, to provide a rough estimate, we assumed that non-street trees would be managed in the same way as street trees (i.e., removal and replacement of dead trees). In this scenario, added mortality would incur an estimated annualized cost of $1.5B for non-residential trees and $356M for residential trees. Further, a disproportionate amount of the total damages (91% of the mortality to residential non-residential community trees) is expected to be felt in the hotspot zone, with 12.1 million residential and 65.9 million non-residential community trees expected to be killed. Given the relatively limited data, and the difference in potential management behaviour for these trees, we caution against overinterpretation of these results.

Novel IAFI risk forecast

Our framework allowed us to identify the factors leading to the greatest impacts for IAFIs already known to have established in the United States. We were able to identify the most common urban host trees, the sites facing the greatest future IAFI propagule pressure, and the IAFI-host combinations with the greatest mortality. However, this approach can also be synthesized with IAFI entry scenarios to understand potential impacts of novel invasive IAFIs. To illustrate the utility of this framework for prediction, we have provided a checklist of risk factors in Table S11 and future spread simulations in Table S12 and Fig. S12. We show that entry via a southern port (e.g., the Port of South Louisiana) would lead to the greatest number of exposed trees. Further, an EAB-like borer of oak and maple trees could kill 6.1 million street trees and cost $4.9B over the next 30 years.

Discussion

While previous analyses have indicated that urban trees are associated with the largest share of economic damages due to IAFIs (Aukema et al. 2011, Paap et al. 2017, Kovacs et al. 2010), until recently, data did not exist on the urban distribution of host trees (Koch et al. 2018), the spread of IAFIs (Hudgins et al. 2017,2020), nor the mortality risk for hosts due to different IAFIs (Potter et al. 2019). With these new models, it is now possible to forecast where and when IAFIs will have the most damages across the US. Our analysis suggests an overall added mortality of between 2.1-2.5% of all street trees, amounting to $US 30M per year in management costs. However, the most interesting and potentially useful element was our ability to forecast hotspots of future forest IAFI damages, including a 902,500km^2 region that we expect to experience 95.7% of all mortality, in large part due to a 98.8% loss of its ash street trees due to EAB. This type of forecasting has been highlighted as a crucial step in prioritizing management funds (McGeoch et al. 2016). These data can be used by municipal pest managers to anticipate future costs, and may help motivate improved spread control programs that aim to identify the potential source counties of future invasions and mitigate the worst anticipated impacts (complete forecast available at http://github.com/emmajhudgins/UStreedamage).

Beyond present IAFI risks, our integrated model can also act as a risk assessment tool for street tree mortality caused by novel IAFIs (Table S11-S12, Fig. S12). While ash trees are assured to be dramatically affected by EAB over the next few decades, our models suggest oak and maple to be the most common street tree genera nationwide.

Further, while ash species are being substituted with less susceptible tree species, maples and oaks continue to be widely planted within our street tree inventories. Therefore, IAFIs with host species spanning these genera should be of heightened concern. Secondly, the timescale and magnitude of the impacts of wood borers (see also Aukema et al. 2011) make them the highest risk to street trees. We integrated these two pieces of information with information on major ports of entry within the US (American Association of Port Authorities 2015, http://aapa.com/), as well as our general model of IAFI spread (Hudgins et al. 2020), to forecast the extent of exposed maple and oak street trees from 2020-2050 (Fig. S12, Table S12). Our analyses show that entry via a southern port would lead to the greatest number of exposed trees. Further, larger trade volumes between the US and Asia compared to other regions (Sardain et al. 2019) suggest Asian natives will be the most likely future established IAFIs. One potential candidate species fitting these criteria is citrus longhorned beetle (*Anoplophora chinensis*), which is an Asian wood borer possessing many potential US host species, including ash, maple and oak (Haack et al. 2010). The lack of more thorough regulation of live plant imports and strict implementation of current wood treatment protocols such as ISPM15 (Lovett et al. 2016) increase the susceptibility of the US to invasion and subsequent spread of this species and other potentially high-risk borers.

Our impact estimates vary substantially based on dynamics of host mortality following initial IAFI invasion, especially because of variability in the duration and functional form of mortality debt. Luckily, the guild (borers) and species (EAB) whose impact on total community costs are most sensitive to correct specification of the mortality debt dynamics are the ones for which we are most confident. Several

423 publications have demonstrated near-complete decimation of ash stands in the decade
424 following EAB infestation (Kovacs et al. 2010, Knight et al. 2013, Fei et al. 2019).
425 Furthermore, since total tree mortality is asymptotically equivalent across all mortality
426 debt regimes, if other feeding guilds possessed 10-year mortality debt regimes, we should
427 have been able to detect a rapid die-off of their hosts as they spread, similarly to what we
428 found for EAB (albeit scaled by their maximum mortality rates). This is not the case in
429 the literature (Fei et al. 2019).

430 With our integrated model, we also estimated economic damages, which updates
431 the decade old Aukema et al. (2011) using recent advances (Koch et al. 2018, Potter et al
432 2019). Surprisingly, the previous cost estimates were not that different at the country
433 scale. The previous cost estimate separated urban trees into residential and non-
434 residential types, grouping street trees in the latter. We estimate annualized costs for non-
435 residential trees to be somewhat lower than those in Aukema et al. (2011, $1.3B versus
436 $2.0B in total “Local Government expenditures”). This lower estimate is likely because
437 of a lower rate of predicted ash exposure to EAB (i.e., lower predicted ash abundance in
438 areas of predicted EAB spread) in non-residential areas. Interestingly, our estimate of
439 residential tree costs is roughly one third that in Aukema et al. (2011, $303M vs $1.1B in
440 total “Household Expenditures”), again likely due to a (more extreme) overestimate in
441 the nationwide prevalence of residential ash trees in the previous publication.

442 We predict that 75% of communities containing ash trees and 68% of all street
443 ash will remain untouched by EAB by 2060 because of the lack of forest ash beyond our
444 forecasted invasion extent, thus limiting exposure. Spatially, our results show lower
445 threat in the western US. This pattern is consistent with previous findings (Lovett et al.

2016) and can be explained by the high impacts of EAB, LDD moth, and hemlock woolly adelgid, whose distributions are projected to concentrate further east in the short term. However, some of the highest-impact non-native pathogens have emerged in the western US and were not captured in this analysis (Kinloch Jr. 2003, Rizzo & Garbelotto 2003). Western regions could also see high future risks due to the polyphagous shot hole borer (*Euwallacea whitfordiodendrus)* and its insect-disease complex with fusarium fungus (*Fusarium spp.*) (Coleman et al. 2019). This complex has already established in California and has maple and oak trees among its many hosts.

While the substantial advances that emerged recently allowed us to develop a more fully integrated model, we also identified data deficiencies which require additional research. A relative quantification of additional sources of uncertainty is provided in Appendix S4. Further, this cost estimate only examines the cutting of dead trees. The analysis fails to account for preventative cutting prior to EAB arrival, to fully examine non-street tree management, and to assess the impacts of IAFIs that have not yet established in the United States. Furthermore, our analysis assumes a complete identification of 'high impact IAFIs'. Some presently established IAFIs may not yet have been identified as 'high impact', either due to lags in their impact, and/or lags in the detection of this impact (Coutts et al. 2018), but may become 'high impact' before 2050.

We have shown that the suite of known IAFIs have the potential to kill roughly a hundred million additional urban trees in the US in the next 30 years. While these numbers themselves are striking, reporting only a country-level impact estimate without IAFI species, tree, and community-level resolution does little to inform management prioritizations. Here, we were able to identify specific urban centers, IAFI species, and

host tree genera associated with the vast majority of these impacts. We predict that 90% of all street tree mortality within the next 30 years will be EAB-induced ash mortality, and that ~95% of all street tree mortality will be concentrated in less than 25% of all communities. These estimates illustrate the gravity of IAFI infestations for communities in the path of high impact invaders that are rich in susceptible hosts. Moreover, we were able to use this framework to identify a checklist of biotic and spatiotemporal risk factors for future high-impact street tree IAFIs.

Acknowledgments

EJH would like to thank her PhD supervisory committee members T. Jonathan Davies and Patrick M. A. James for their invaluable comments, as well as the thoughtful comments and questions from thesis external examiner Dominique Gravel and colleague Andrew Liebhold. EJH also acknowledges the continual support and feedback from lab members Dat Nguyen, Abbie Gail Jones, Charlotte Steeves, Shriram Varadarajan, and Lidia Della Venezia. This work was supported by a NSERC CGS-D awarded to EJH. This research was funded, in part, through Cost Share Agreements 17-CS-11330110-025, 18-CS-11330110-026, and 19-CS-11330110-027, between the USDA Forest Service and North Carolina State University.

References

Aukema, J. E., Leung, B., Kovacs, K., Chivers, C., Britton, K. O., Englin, J., ... *et al.* (2011). Economic impacts of non-native forest insects in the continental United States. *PLoS One*, 6(9).

Aukema, J. E., McCullough, D. G., Von Holle, B., Liebhold, A. M., Britton, K., & Frankel, S. J. (2010). Historical accumulation of nonindigenous forest pests in the continental United States. *BioScience*, 60(11), 886-897.

Carpenter, B., Gelman, A., Hoffman, M. D., Lee, D., Goodrich, B., Betancourt, M., ... *et al*. (2017). Stan: A probabilistic programming language. *J Stat. Soft.*, 76(1).

Coleman, T. W., Poloni, A. L., Chen, Y., Thu, P. Q., Li, Q., Sun, J., ... *et al.* (2019). Hardwood injury and mortality associated with two shot hole borers, Euwallacea

497 spp., in the invaded region of southern California, USA, and the native region of
498 Southeast Asia. *Ann. Forest Sc.i*, 76(3), 1-18.
499 Coutts, S. R., Helmstedt, K. J., & Bennett, J. R. (2018). Invasion lags: The stories we tell
500 ourselves and our inability to infer process from pattern. *Divers. Distrib*, 24(2),
501 244-251.
502 Fahrner, S. J., Abrahamson, M., Venette, R. C., & Aukema, B. H. (2017). Strategic
503 removal of host trees in isolated, satellite infestations of emerald ash borer can
504 reduce population growth. *Urban For. Urban Green.*, 24, 184-194.
505 Fei, S., Morin, R. S., Oswalt, C. M., & Liebhold, A. M. (2019). Biomass losses resulting
506 from insect and disease invasions in US forests. *Proc. Natl. Acad. Sci.* 116(35),
507 17371-17376.
508 Fick, S. E., & Hijmans, R. J. (2017). WorldClim 2: new 1-km spatial resolution climate
509 surfaces for global land areas. *Int. J Climatol.*, 37(12), 4302-4315.
510 Haack, R. A., Hérard, F., Sun, J., & Turgeon, J. J. (2010). Managing invasive populations
511 of Asian longhorned beetle and citrus longhorned beetle: a worldwide
512 perspective. *Ann. Rev. Entomol.*, *55*.
513 Hijmans, R. J., Phillips, S., Leathwick, J., Elith, J., & Hijmans, M. R. J. (2017). Package
514 'dismo'. *Circles*, 9(1), 1-68.
515 Homer, C.G., Dewitz, J.A., Yang, L., Jin, S., Danielson, P., Xian, G., … *et al*. (2015.)
516 Completion of the 2011 National Land Cover Database for the conterminous
517 United States – representing a decade of land cover change information.
518 *Photogramm. Eng. Remote Sensing*, 81, 345–354.
519 Hudgins, E. J., Liebhold, A. M., & Leung, B. (2017). Predicting the spread of all invasive
520 forest pests in the United States. *Ecol. Lett.*, 20(4), 426-435.
521 Hudgins, E. J., Liebhold, A. M., & Leung, B. (2020). Comparing generalized and
522 customized spread models for nonnative forest pests. *Ecol. Appl.*, 30(1), e01988.
523 Hulme, P. E. (2009). Trade, transport and trouble: managing invasive species pathways in
524 an era of globalization. *J Appl. Ecol.*, 46(1), 10-18.
525 IPPC (International Plant Protection Convention). 2002. International standards for
526 phytosanitary measures. Rome, Italy: FAO.
527 www.fao.org/docrep/009/a0450e/a0450e00.htm. Viewed 12 May 2020.
528 Kinloch Jr, B. B. (2003). White pine blister rust in North America: past and
529 prognosis. *Phytopathol.*, 93(8), 1044-1047.
530 Knight, K. S., Brown, J. P., & Long, R. P. (2013). Factors affecting the survival of ash
531 (*Fraxinus* spp.) trees infested by emerald ash borer (*Agrilus planipennis*). *Biol.*
532 *Invasions*, 15(2), 371-383.
533 Koch, F. H., Ambrose, M. J., Yemshanov, D., Wiseman, P. E., & Cowett, F. D. (2018).
534 Modeling urban distributions of host trees for invasive forest insects in the eastern
535 and central USA: A three-step approach using field inventory data. *Forest Ecol.*
536 *Manage.*, 417, 222-236.
537 Kovacs, K. F., Haight, R. G., McCullough, D. G., Mercader, R. J., Siegert, N. W., &
538 Liebhold, A. M. (2010). Cost of potential emerald ash borer damage in US
539 communities, 2009–2019. *Ecol. Econ.*, 69(3), 569-578.
540 Kovacs, K., Václavík, T., Haight, R. G., Pang, A., Cunniffe, N. J., Gilligan, C. A., &
541 Meentemeyer, R. K. (2011). Predicting the economic costs and property value

losses attributed to sudden oak death damage in California (2010–2020). *J Environ. Manage.*, 92(4), 1292-1302.

Leung, B., Springborn, M. R., Turner, J. A., & Brockerhoff, E. G. (2014). Pathway-level risk analysis: the net present value of an invasive species policy in the US. *Front. Ecol. Environ.*, *12*(5), 273-279.

Lovett, G. M., Weiss, M., Liebhold, A. M., Holmes, T. P., Leung, B., Lambert, K. F., ... & Weldy, T. (2016). Nonnative forest insects and pathogens in the United States: Impacts and policy options. *Ecol. Appl.*, *26*(5), 1437-1455.

McGeoch, M. A., Genovesi, P., Bellingham, P. J., Costello, M. J., McGrannachan, C., & Sheppard, A. (2016). Prioritizing species, pathways, and sites to achieve conservation targets for biological invasion. *Biol. Invasions*, 18(2), 299-314.

Norton, B. A., Coutts, A. M., Livesley, S. J., Harris, R. J., Hunter, A. M., & Williams, N. S. (2015). Planning for cooler cities: A framework to prioritise green infrastructure to mitigate high temperatures in urban landscapes. *Landsc. Urban Plan.*, 134, 127-138.

Paap, T., Burgess, T. I., & Wingfield, M. J. (2017). Urban trees: bridge-heads for forest pest invasions and sentinels for early detection. *Biol. Invasions*, 19(12), 3515-3526.

Potter, K. M., Escanferla, M. E., Jetton, R. M., & Man, G. (2019). Important insect and disease threats to United States tree species and geographic patterns of their potential impacts. *Forests*, 10(4), 304.

Pugh, S.A. (2010). *Michigan's forest resources, 2008.* Research Note NRS-50. Newtown Square, PA: U.S. Forest Service, Northern Research Station. 4 pp.

Rizzo, D. M., & Garbelotto, M. (2003). Sudden oak death: endangering California and Oregon forest ecosystems. *Front. Ecol. Environ.*, 1(4), 197-204.

Roy, S., Byrne, J., & Pickering, C. (2012). A systematic quantitative review of urban tree benefits, costs, and assessment methods across cities in different climatic zones. *Urban For. Urban Green.*, 11(4), 351-363.

Sardain, A., Sardain, E., & Leung, B. (2019). Global forecasts of shipping traffic and biological invasions to 2050. *Nat. Sust.*, 2(4), 274-282.

Van den Berg, A. E., Maas, J., Verheij, R. A., & Groenewegen, P. P. (2010). Green space as a buffer between stressful life events and health. *Soc. Sci. Med.*, 70(8), 1203-1210.

Figures

Figure 1. Fit of the genus-specific host tree models across all genera and size classes.

Figure 2. Model outputs for the first three subcomponent models, including **a.** predicted street tree abundance, **b.** predicted newly invaded sites of existing IAFIs, **c.** predicted street tree exposure levels (number of focal host tree + IAFI interactions) from 2020 to 2050, and finally **d.** Predicted total tree mortality from 2020 to 2050 in the most likely mortality debt scenario across space. The top seven most impacted cities or groups of nearby cities are shown in terms of total tree mortality 2020 to 2050 (A = Milwaukee, WI; B = Chicago/Aurora/Naperville/Arlington Heights, IL; C = New York, NY; D = Seattle, WA; E = Indianapolis, IN; F = Cleveland, OH; G = Philadelphia, PA).

Figure 3. Posterior distribution for the beta model of host mortality due to IAFIs within each severity category. 95% Bayesian credible intervals are shown in grey, and the posterior median is shown in black. Colored bins represent severity categories extended from Potter et al. (2019).

Figure 4. Depiction of the influence of mortality debt on temporal cost patterns. Predicted costs 2020 to 2050 for the 10 year (yellow), 50 year (teal), and 100 year (purple) mortality debt scenarios with a 10 year initial invasion lag. The most likely scenario predictions are shown as a dashed red line. Costs are presented in 5-year increments in accordance with the timestep length within our spread model.

597 **Figure 1**

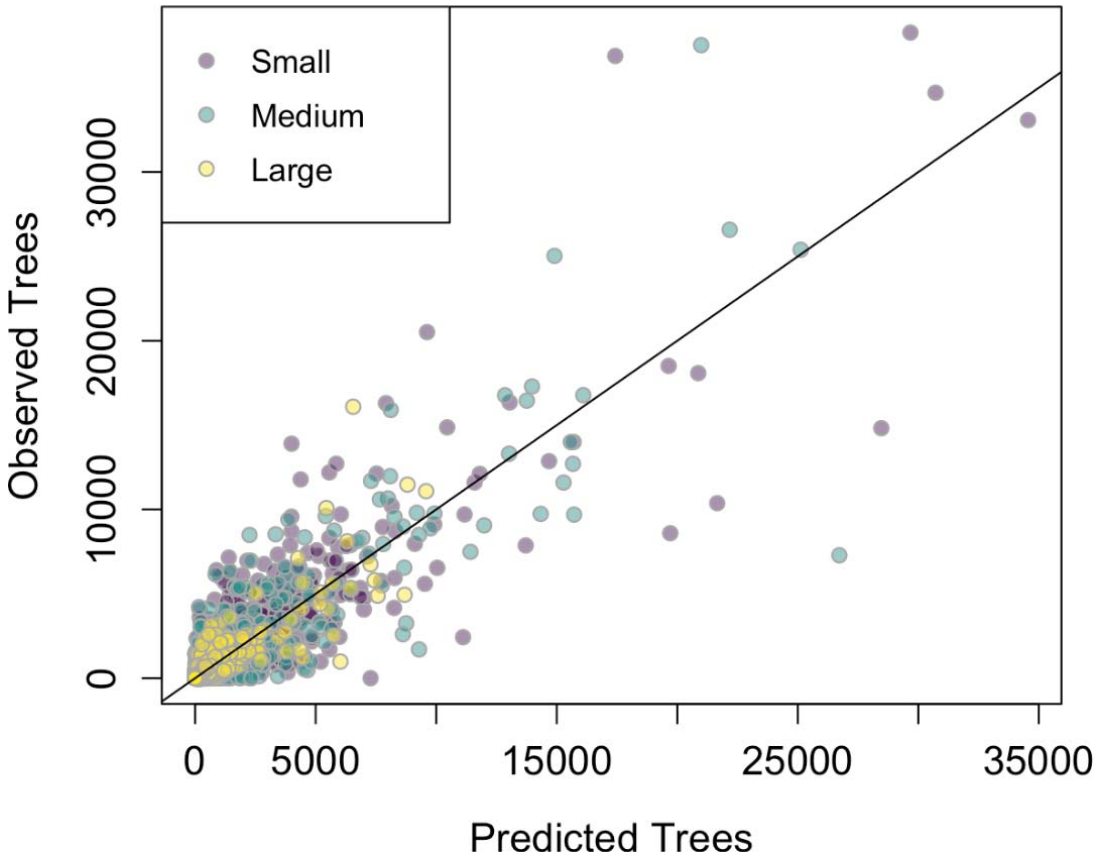

598

599

600 **Figure 2**

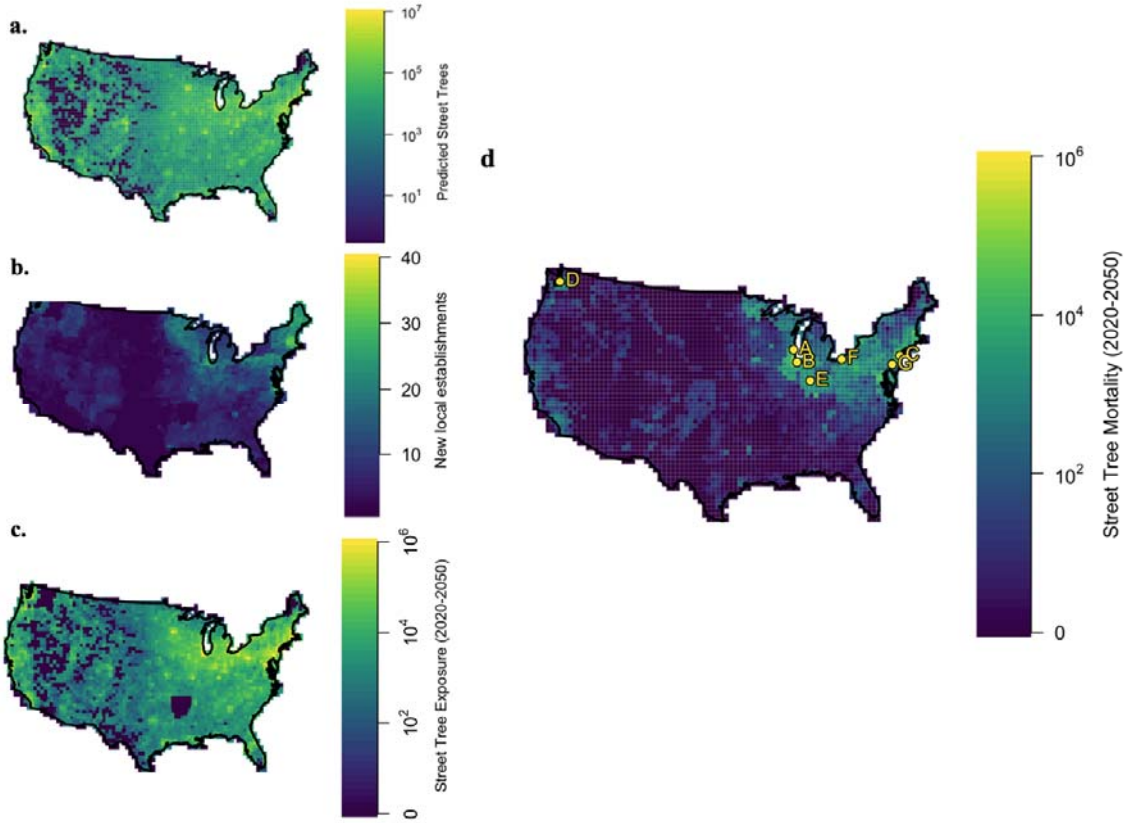

601
602

603 **Figure 3**

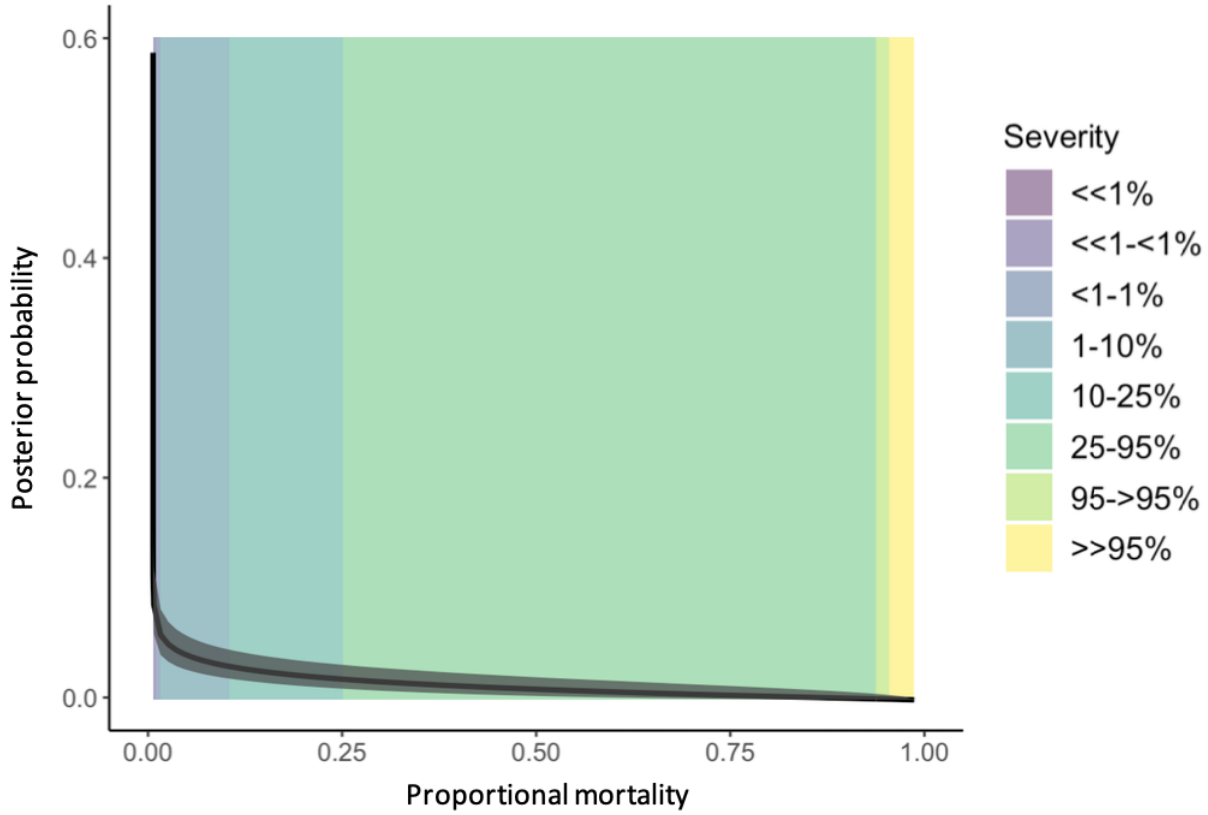

604

605

606 **Figure 4**

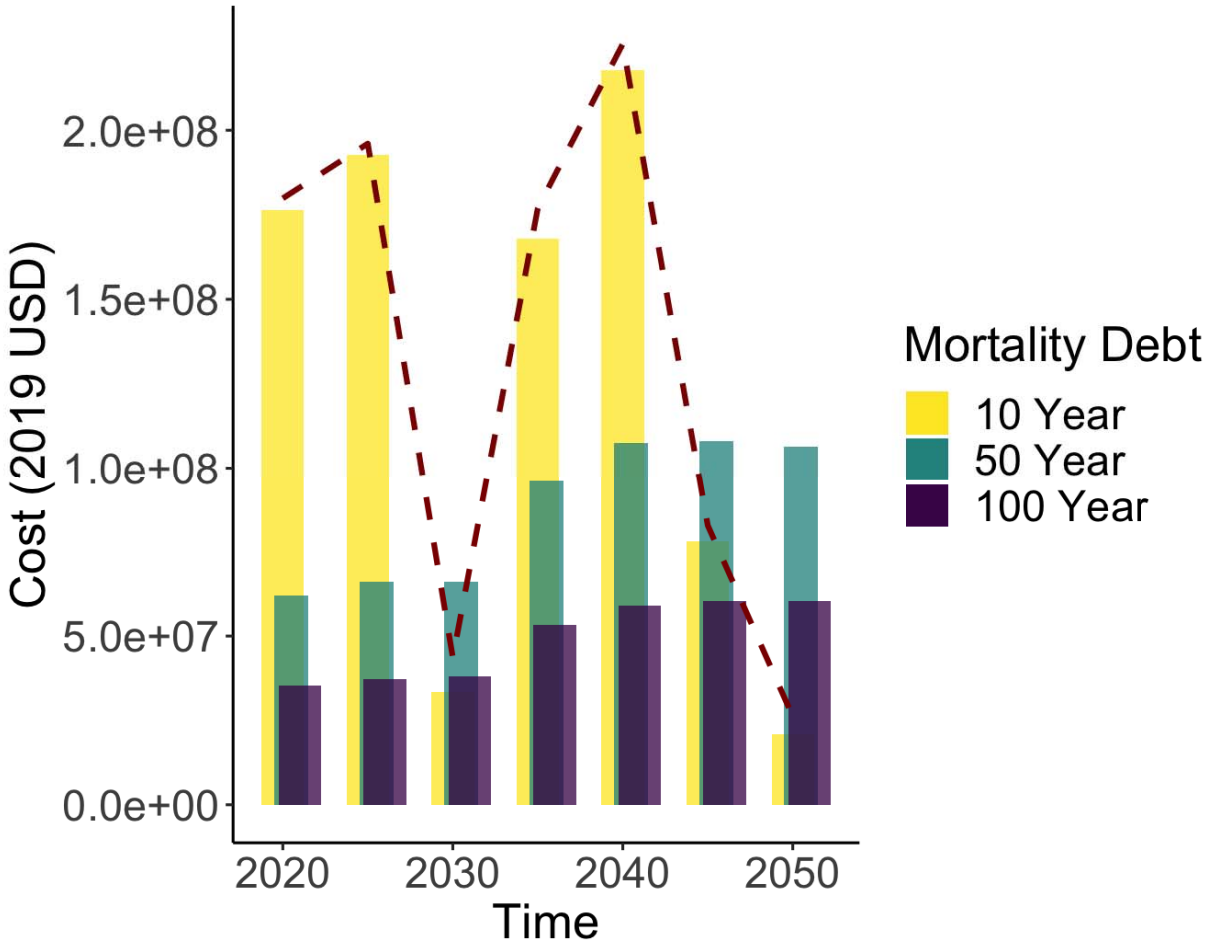

607
608

609 ## Tables
610
611 **Table 1.** Predicted annualized cost (in 2019 US dollars) and tree mortality across
612 invasion scenarios from 2020 to 2050 across all 57 IAFI species. “Most likely” indicates
613 the scenario with expert-elicited mortality debt durations by feeding guild, “Vary”
614 scenarios hold all guilds but the focal guild constant at their most likely scenario, and
615 “All” fix all three guilds at a given mortality debt duration. Mean mortality for most
616 likely scenario = 2.3%, 1.38M trees, US$ 30M annualized (US$ 679M over the next 30
617 years).
618

Mortality Debt Scenario	**Annualized Cost (US$ millions)**		**Tree Mortality (Millions)**		**Percent Mortality**	
	lower 95% CI	upper 95% CI	lower 95% CI	upper 95% CI	lower 95% CI	upper 95% CI
Most likely	28.5	33.2	1.29	1.54	2.1%	2.5%
Vary Borers	10.1	32.1	0.45	1.45	0.7%	2.4%
Vary Defoliators	28.1	32.6	1.28	1.48	2.1%	2.4%
Vary Sap-feeders	28.5	32.5	1.30	1.47	2.1%	2.4%
All 10	27.8	30.4	1.27	1.39	2.1%	2.3%
All 50	18.5	22.3	0.84	1.00	1.4%	1.7%
All 100	9.77	13.5	0.44	0.60	0.7%	1.0%

619